Insights into the structure and evolution of large volcanoes on Venus from high-resolution stereo-derived topography. K. R. Verner[1], G. A. Galgana[2], P. J. McGovern[2], and R. R. Herrick[3], [1]Huffington Department of Earth Sciences, Southern Methodist University, Dallas, TX 75275, USA (kverner@smu.edu), [2]Lunar and Planetary Institute, 3600 Bay Area Blvd., Houston, TX, 77058, USA (galgana@lpi.usra.edu, mcgovern@lpi.usra.edu), [3]Department of Geology and Geophysics, University of Alaska Fairbanks, Fairbanks, AK 99775, USA.

Introduction: The Magellan mission to Venus provided 98% global coverage of synthetic aperture radar imagery and nadir-looking altimeter data. The study of volcanoes has been hampered by lack of high-resolution topography data (10-20 km horizontal resolution). This is sufficient in capturing broad-scale edifices, but moderate- to small-scale tectonic features are poorly or not at all resolved. Smaller surface features offer important constraints on volcanic processes: sub-surface storage, movement of magma, and lithospheric flexure on the state of stress in the edifice [1, 2]. We study surficial strain patterns to understand these volcanic processes.

Data: The digital elevation models (DEMs) used in this study are derived from Magellan stereo images and have 1-3 km horizontal resolution [3,4]. Several volcanic edifices can be structurally analyzed because of their extensional radial fault systems, giving hints to the origin and modes of magma emplacement [5]. We focus on seven volcanic systems that exhibit a sufficient number of radial and circumferential faults. These volcanic systems include Kunapipi, Anala, Irnini, Gula and Didilia Montes, and Pavlova and H'uraru Coronae. Measurements were taken on the merged GTDR and stereo DEM datasets, along with the raw and filtered versions of each DEM.

Methods: We used the image processing software ENVI to create 3D visualizations of volcanic features, combining the left-view backscatter images with the stereo DEMs. This helped us determine which faults/fractures have sufficient offsets that would be useful for structural interpretation. To provide accurate measurements, strike-trending profiles were taken along identified faults and fractures, supplemented by perpendicular cross-sections. Topographic profiles based on the high-pass filtered digital elevation models (DEM_H) were used in measuring the throw of faults and fractures. Extension was determined by:

$$\Delta W = h/\tan\Theta$$

where ΔW is the minimum amount of extension, h is the depth of the fault and Θ is the fault dip angle (taken to be 60° to represent the original fault surface strain for a normal fault). The hoop strain was calculated by summing the extension measurements and dividing by the circumference around the RFC:

$$\varepsilon(r) = \Sigma\Delta W(r)/2\pi r$$

where r is the radius from center. These measurements could then be used as quantitative constraints to identify volcano-tectonic processes that have contributed to edifice development.

We used MATLAB inversion codes to determine the best-fit reservoir geometry, comparing observed with modeled strains. In particular, we compute radial and vertical strains due to: a) an inflating spherical magmatic source [6] and b) due to a penny-crack, sill-like magma chamber.

Results: We note significant improvement in the interpretability of structural features in the images, as the combined display of topography and backscatter images enable precise measurement of fracture openings and fault offsets in three dimensions. In particular, the improved DEM of Anala Mons gives new perspectives on the nature of flank-trending faults and how these are related to the structural development of these volcanoes (Figures 1). In the case of Anala Mons, the NNE-SSW trending, summit-crossing fracture system show considerable fault throws that indicate the large deformation events undergone by the summit during its development (Figures 1 & 2).

Our inversions at Anala Mons show that a penny crack/sill-like magma chamber situated at the center of these volcanoes (at depths = 10 km) fit the deformation patterns. The dimensions of a spherical reservoir cannot produce these deformations.

Discussion. Improvement on the resolution of topographic features found on volcanic edifices are critical to structural interpretation and affects the modeling process, enabling new techniques to

quantify volcano deformation and trace the origin and pathways of magma. Preliminary inversion processes resolve the location of sill-like magmatic sources responsible for the deformation of these edifices (Figure 3).

References: [1] Grosfils E. and J. Head (1994), *GRL*, 21(8) :701-704. [2] McGovern P. and S. Solomon (1998), *JGR*, 103:11, 071-11,101. [3] Gleason, A. et al. (2010). *JGR*, 115, E06004, doi:10.1029/2009JE003431. [4] Herrick, R. et al. (2010), *LPSC*, Abstract 1622. [5] Janes, D. and S. Squyres (1993), *GRL*, 20(24): 2,961-2,964. [6] McTigue, D. (1987). *JGR*, 92(B12): 12,931-12,940. [7] Grindrod, P. et al. (2005), *JGR*, 110, E12002, doi:10.1029/2005 JE002416.

A)

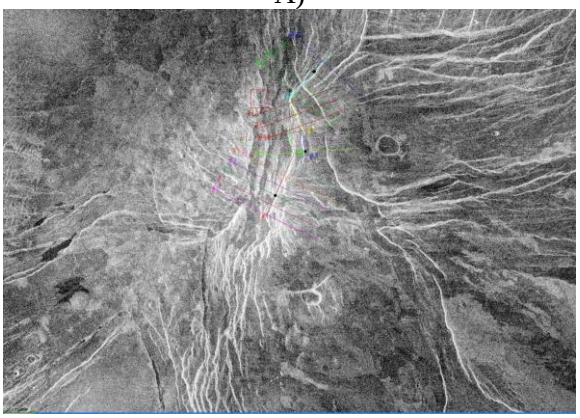

B)

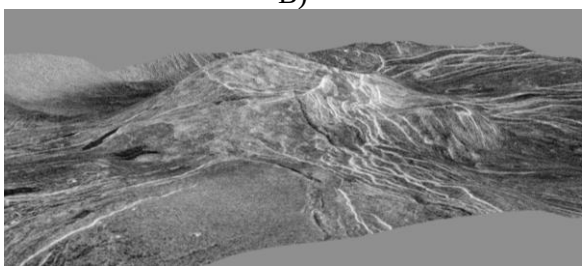

C)

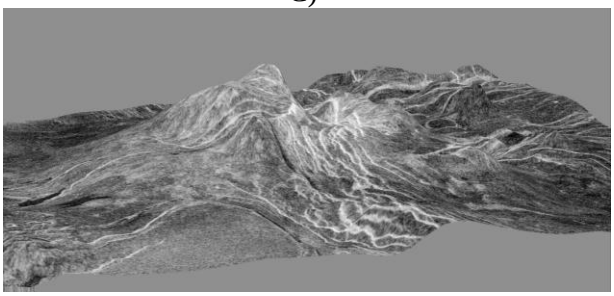

Figure 1: (A) Magellan left-viewing back-scatter image of Anala Mons, showing extensive radiating fractures through its summit; (B): Backscatter image draped on GTDR dataset, showing Anala Mons summit, in perspective view (view towards the northeast). Vertical exaggeration (VE) = 20x ; and (C): Backscatter image of Anala Mons draped over stereo dataset in perspective view (view towards northeast), revealing summit depression produced by rift-like fracture, VE = 20x.

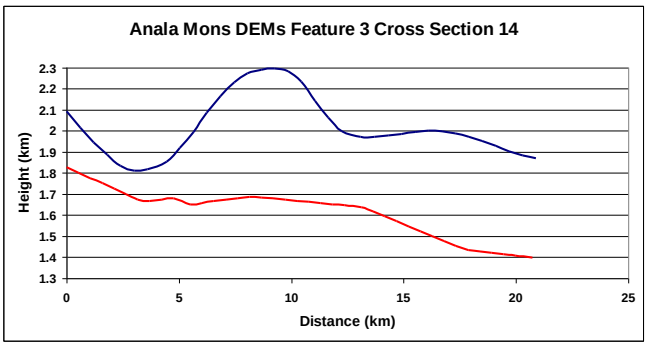

Figure 2. Topographic cross–section #14 from feature 3 on Anala Mons. Blue line shows topography for DEM_H and red line shows topography for DEM_G. DEM_H is offset from DEM_G by about 230m.

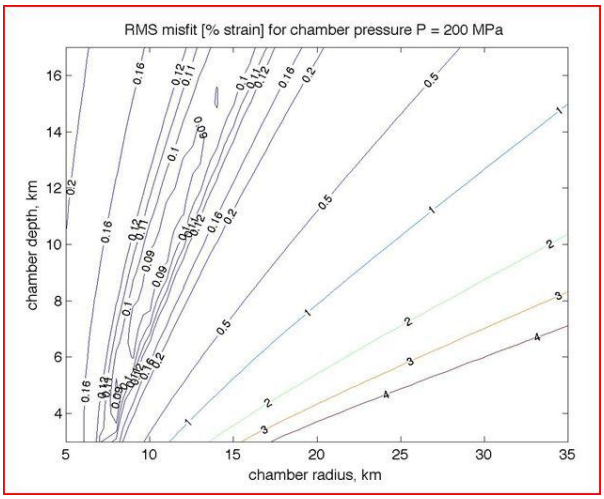

Figure 3. RMS misfit [% strain] for chamber pressure P = 200 MPa, for a sill-like magma chamber.